ORGANIC CHEMISTRY FRONTIERS

RESEARCH ARTICLE

View Article Online
View Journal | View Issue

Cite this: *Org. Chem. Front.*, 2023, **10**, 42

Precise control of the site selectivity in ruthenium-catalyzed C–H bond amidations using cyclic amides as powerful directing groups†

Yu-Chao Yuan, *[a] Qiu-Li Lu,[a] Xiao-Tong Zhu,[a] Sergio Posada-Pérez,[b] Miquel Solà,[b] Albert Poater, *[b] Thierry Roisnel[c] and Rafael Gramage-Doria *[c]

Selective C–H functionalizations aiming at the formation of new C–N bonds is of paramount importance in the context of step- and atom-economy methodologies in organic synthesis. Although the implementation of noble metal catalysts is prevalent, more benign cobalt pre-catalysts have recently appeared to be promising. However, they sometimes feature selectivity issues that limit their applicability in late-stage functionalization. Herein, we report on a highly reactive ruthenium-based catalytic system displaying excellent levels of mono-, regio- and site-selectivity by exploiting a series of biologically-relevant cyclic amides as weak directing groups. The use of dioxazolone derivatives as amidating reagents overcomes the issues encountered in the use of unstable azide derivatives for such transformations and it enables us to perform these reactions under very mild reaction conditions (air, 40 °C). Moreover, a combination of deuteration experiments and a comparative study with different types of directing groups highlights the relevance of weak amide directing groups for enabling the formation of six-membered cycloruthenate intermediates in the key elementary steps of the catalytic cycle. In addition, DFT computational calculations were carried out for the first time for studying ruthenium-catalyzed C–N bond-forming processes *via* C–H activation assisted by weak directing groups, thereby elucidating the origin of the regio- and site-selectivity.

Received 8th September 2022,
Accepted 3rd November 2022

DOI: 10.1039/d2qo01434c

rsc.li/frontiers-organic

Introduction

The selective formation of C–heteroatom bonds is a fundamental transformation with direct consequences in the streaming synthesis of highly elaborated molecules with important applications ranging from pharmacology to materials science.[1] In this context, C–N bond-forming processes are significantly relevant as they can be targeted in a sustainable manner using transition metal complexes as homogeneous catalysts.[2] From the pioneering discoveries of the Ullmann coupling with copper catalysts[3] to the most recent Buchwald–Hartwig aminations with palladium ones,[4] these and analogous transformations have completely revolutionized the way of conceiving organic synthesis.[5] However, most of these protocols require the use of pre-activated starting materials which impose synthetic limitations together with undesired over-stoichiometric formation of hazardous byproducts.[3–5] Consequently, new promising approaches based on transition metal-catalyzed C–H bond functionalizations have appeared in the last few decades for amination reactions that can directly be performed on low functionalized starting materials.[6] In this scenario, the selectivity is typically controlled by the presence of a directing group (DG) nearby the C–H bond desired to be functionalized.[7] Therefore, this leads typically to *ortho*-selectivity for aromatic C–H bond aminations[7] although few cases of remote *meta*- and *para*-C–H bond aminations have been reported.[8]

Among many known C–N bond-forming reactions, transition metal-catalyzed *ortho*-C–H amidation ones are particularly interesting given the ubiquitous nature of amide bonds.[9,10] Catalysts based on Ir, Rh, Pd, Ru or Co are of choice due to their high reactivity[11] and amidating agents derived from dioxazolone are preferred instead of azides because of their benchmark stability.[12] Taking this into account, it appears that all reports from the literature dealing with transition metal-catalyzed C–H bond amidations focused exclusively on substrates containing only one aromatic C–H bond

[a]*Jiangsu Key Laboratory of New Drug Research and Clinical Pharmacy, School of Pharmacy, Xuzhou Medical University, Xuzhou 221004, China. E-mail: yuchao.yuan@xzhmu.edu.cn*
[b]*Institut de Química Computacional i Catàlisi and Departament de Química, Universitat de Girona, C/M. Aurèlia Capmany, 17003 Girona, Catalonia, Spain. E-mail: albert.poater@udg.edu*
[c]*Univ Rennes, CNRS, ISCR – UMR6226, F-35000 Rennes, France. E-mail: rafael.gramage-doria@univ-rennes1.fr*

†Electronic supplementary information (ESI) available. CCDC 2149748. For ESI and crystallographic data in CIF or other electronic format see DOI: https://doi.org/10.1039/d2qo01434c

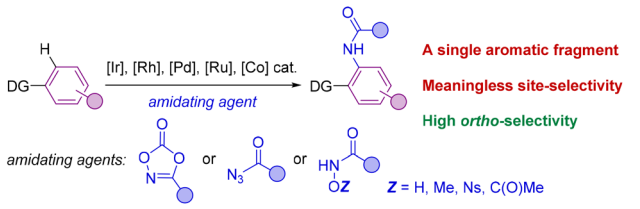

Scheme 1 General case of a transition metal-catalyzed C–H bond amidation on aromatic scaffolds. DG = directing groups.

available for reaction (Scheme 1).[7,11,12] However, for implementation in late-stage functionalization for instance, the methodologies may consider also the compatibility with other aromatic C–H bonds prone to react. Unfortunately, the site-selectivity of aromatic C–H bond amidation reactions has been rarely studied to date with low levels of selectivity so far reported. In a first study in 2017, Chang and co-workers demonstrated for a single example (*N*-phenylbenzamide) that a C–H bond amidation could be site-selective with a cobalt catalyst and unproductive with a ruthenium catalyst, albeit with a modest yield (Scheme 2A).[11d] Later, Whiteoak and co-workers showed, as it could be expected, that a statistical mixture of amidated products is obtained using a cobalt catalyst with the assistance of an acyclic amide directing group in yields not exceeding 30% (Scheme 2B).[13]

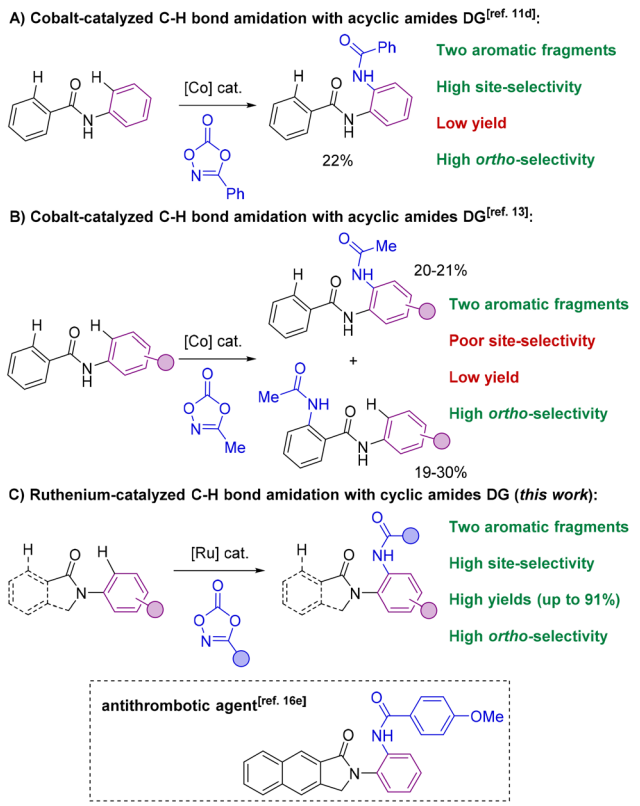

Scheme 2 Transition metal-catalyzed C–H bond amidations on aromatic scaffolds using amides as directing groups: the state-of-the-art (A and B) *versus* present work (C).

These examples undoubtedly show the difficulty in achieving site-selective C–H bond amidations in the presence of multiple aromatic fragments. Herein, we show that both regio- and site-selectivities are achieved when using cyclic amides as directing groups in the presence of two aromatic sites prone to react by means of a ruthenium catalyst that additionally displays broad functional group tolerance (Scheme 2C). We found that *ortho*-C–H bond amidations selectively took place in the *N*-aryl fragment rather than in the *C*(O)-aryl site. Control experiments, preliminary mechanistic studies and thorough DFT calculations unambiguously support that cyclic amides enable the formation of catalytically productive six-membered ruthenacycles as unique intermediates[14] as it was evoked but never demonstrated in C–O and C–C bond forming reactions.[15] It is noteworthy that cyclic amides, such as isoindolinones employed in this study, are prevalent motifs encountered in several daily-life chemicals (Scheme 2C, framed);[16] therefore the presented methodology paves the way towards the use of ruthenium catalysts in C–H bond late-stage functionalization strategies.[17] An in-depth comparative study with other types of common directing groups is presented, indicating the suitability of weak amide directing groups over more coordinating ones, such as pyridines, for ruthenium-catalyzed C–H bond amidations. In addition, cyclic amides were found to outperform acyclic ones as directing groups in this relevant transformation.

Results and discussion

Our initial efforts started by using *N*-arylisoindolinone (**1a**) as the model substrate for the optimization of the C–H bond amidation reaction with 3-phenyl-1,4,2-dioxazol-5-one (**2a**) as the amidating agent in the presence of $[RuCl_2(p\text{-cymene})]_2$ as the pre-catalyst. After screening a number of parameters (Table 1 and Table S1 in the ESI†), we found suitable reaction conditions that afforded exclusively the amide derivative **3a**, in which the C–H bond amidation occurred in the hydrogen atom Ha (*ortho* position with respect to the nitrogen atom). The C–H bond functionalization taking place at the other possible hydrogen atom Hb was not observed (Table 1). The reaction conditions consisted of 5 mol% $[RuCl_2(p\text{-cymene})]_2$, $AgSbF_6$ as a chloride scavenger, and PivOH as an additive in 2,2,2-trifluoroethanol (TFE) as the solvent at 40 °C under air for 24 hours (Table 1, entry 1). In this way, **3a** was obtained in 80% isolated yield. Control experiments indicated the need for both the chloride scavenger $AgSbF_6$ and the ruthenium pre-catalyst (Table 1, entries 2 and 3). Additives influenced in a different manner the reactivity and selectivity of the C–H bond amidation reaction. Among the different protic additives evaluated, PivOH was found to be the most suitable one (Table 1, entries 4–7). Screening other solvents such as 1,2-dichloroethane (DCE), 1,4-dioxane and tetrahydrofuran (THF) was detrimental to the catalysis compared to TFE (Table 1, entries

Table 1 Optimization of the site-selective ruthenium-catalyzed *ortho*-C–H bond amidation of **1a** with dioxazolone **2a**.[a]

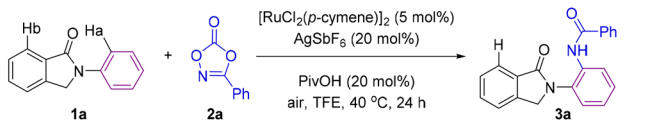

Entry	Deviation from the above conditions	**3a** [b] (%)
1	None	82 (80)[c]
2	No $[RuCl_2(p\text{-cymene})]_2$	0
3	No $AgSbF_6$	0
4	No PivOH	73
5	AcOH instead of PivOH	76
6	$AdCO_2H$ instead of PivOH	79
7	H_2O instead of PivOH	54
8	DCE instead of TFE	65
9	1,4-Dioxane instead of TFE	0
10[d]	THF instead of TFE	19
11	1.2 equiv. of **2a**	60
12	25 °C instead of 40 °C	70
13	$Cp^*Co(CO)I_2$ instead of $[RuCl_2(p\text{-cymene})]_2$	0
14[e]	TsN_3 instead of **2a**	Traces

[a] Reaction conditions: **1a** (0.1 mmol), **2a** (0.15 mmol), $[RuCl_2(p\text{-cymene})]_2$ (5 mol%), $AgSbF_6$ (20 mol%), PivOH (0.02 mmol, 0.2 equiv.), TFE (0.5 mL), 40 °C, 20 h, air. [b] Determined by ^1H NMR spectroscopy against dibromomethane as an internal standard. [c] Isolated yield shown in the parentheses after purification by column chromatography. [d] Reaction performed without PivOH. [e] The product for this reaction is expected to bear a NHTs in place of a NHCOPh fragment in **3a**.

8–10). Lowering the loading of the amidating agent **2a** to 1.2 equivalents afforded the corresponding amidated product **3a** in a modest 60% yield (Table 1, entry 11). Gratifyingly, we found that when decreasing the temperature to room temperature, 70% yield of **3a** was obtained in a reaction conducted at an ambient temperature of 25 °C (Table 1, entry 12). Swapping the ruthenium pre-catalyst with a cobalt complex largely used in C–H bond amidations[13] did not afford any product so far (Table 1, entry 13). The use of tosyl azide (TsN_3), which is a well-known nitrene source,[7] as an amidating agent led to traces of the corresponding *N*-tosylated product analogue of **3a** (NHTs instead of NHCOPh, Table 1, entry 14). Overall, these findings highlight the suitability of ruthenium catalysts over the more expensive iridium, palladium or rhodium ones,[18] as well as dioxazolone **2a** as an ideal and safe partner for this type of transformation.

After reaction optimization (Table 1, entry 1), the scope of the catalysis was evaluated with different synthetically useful functional groups at different positions in both compound **1** and the dioxazolone partner **2** (Table 2). *para*-Substitution patterns in the *N*-phenyl ring with electron-donating groups, such as methyl and methoxy, were tolerated for the catalysis, yielding the corresponding *ortho*-amidated products **3b** and **3c** in 76% and 83% yields, respectively. In addition, X-ray diffraction studies performed on the single crystals of **3c** (Table 2) established without ambiguity the site- and regio-selectivity observed in this C–H bond amidation reaction.[19] Similarly, introduction of electron-withdrawing groups at the *para*-position such as fluoro and ester groups was also tolerated by the catalysis and afforded the corresponding *ortho*-amidated products **3d** and **3e** in 45% and 66% isolated yields, respectively. Notably, although ester groups have been identified as suitable directing groups in several ruthenium-catalyzed C–H bond activations,[20] in the case of **3e**, it is the cyclic amide group (and not the ester group) which dictates the exclusive site-selectivity observed in the C–H bond amidation. Other halide groups such as chloro and bromo were compatible leading to products **3f** and **3g** in 62% and 73% yields, which is relevant for further derivatization sequences by cross-coupling chemistry.[21] Methyl- and methoxy-substituted isoindolinones at the *meta* position of the *N*-phenyl ring afforded the *ortho*-amidated products **3h** and **3i** in 81% and 90% yield, respectively, in a selective manner, without any functionalization occurring at the other *ortho*-C–H bond positions. Analogously, the catalysis was found to be compatible with a significant number of functional groups attached to the dioxazolone core. For instance, aryl-substituted dioxazolone derivatives bearing either electron-donating or electron-withdrawing groups at the *para* position such as methyl, *tert*-butyl, trifluoromethyl and chloro reacted smoothly with **1a**, affording the corresponding *ortho*-C–H bond amidated products **3j**–**3m** in an excellent range of 83–92% isolated yields. Electron deficient substituents on the aryl-substituted dioxazolone such as 3-Cl were also tolerated under the developed catalysis leading to the amidated product **3n** in a remarkable 91% yield, which makes the halide site available for post-functionalization.[21] Multisubstituted groups on the dioxazolone partner were also employed in this catalysis as shown in the successful synthesis of compound **3o** in 66% yield that contains two chloride substituents at both *meta* positions. Additionally, the reaction was also compatible with a very bulky polycyclic aromatic hydrocarbon fragment such as 1-naphthalene substituted dioxazolone leading to **3p** in 38% yield. Interestingly, heteroaromatic-containing amidating agents can also be employed. In the case of a furan-containing dioxazolone, the corresponding product (**3q**) was obtained in 32% yield. However, the more coordinating thiophene one inhibited the catalysis. Gratifyingly, further exploration of the scope of this C–H bond amidation reaction revealed that the aliphatic-substituted dioxazolones were also reactive. For instance, methyl-, *tert*-butyl- and *n*-heptyl-substituted dioxazolones led to the *ortho*-C–H bond amidated products **3r**, **3s** and **3t** in 80%, 76% and 80% yields, respectively.

Overall, a panel of more than twenty different functional groups at different positions around both reagents **1** and **2** were tolerated with no products resulting from other site- and/or regio-selectivity. The absence of bis-*ortho*-amidated products might be rationalized by a plausible intramolecular hydrogen bonding between the NH group from the amide and the carbonyl group from the directing group that forbids the second *ortho*-C–H bond amidation.[22] We additionally noted that the catalysis was sensitive to the steric hindrance found in the coupling partners as evidenced by the lack of reactivity observed for the *ortho*-tolyl derivative from **1** and the *ortho*-chloro-containing aryl-substituted dioxazolone derived from **2**,

Table 2 Evaluation of the scope for the ruthenium-catalyzed *ortho*-C–H bond amidation of both **1** and dioxazolone **2**[a,b]

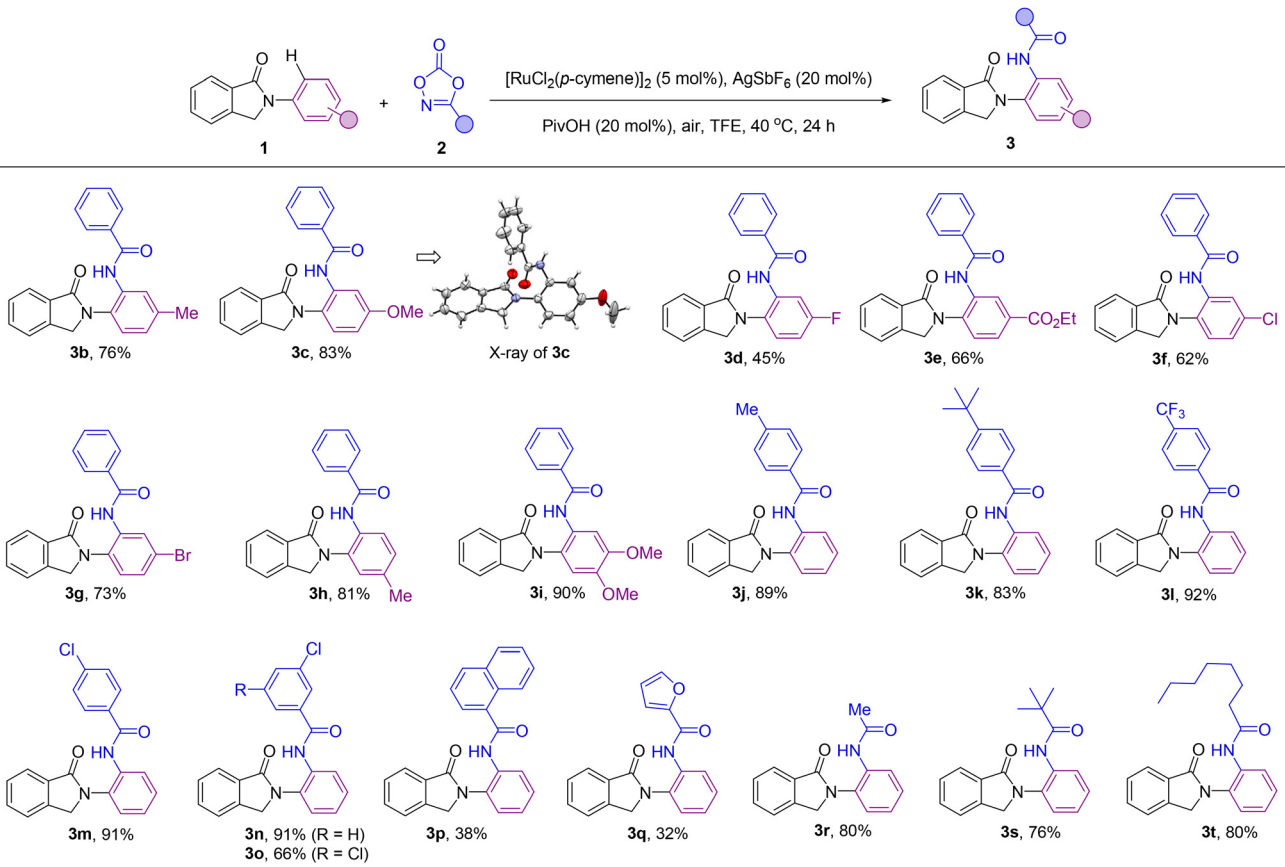

[a] Reaction conditions: **1** (0.3 mmol), **2** (0.45 mmol), $[RuCl_2(p\text{-cymene})]_2$ (5 mol%), $AgSbF_6$ (20 mol%), PivOH (0.06 mmol, 0.2 equiv.), TFE (1.5 mL), 40 °C, 20 h, air. [b] Isolated yield by column chromatography.

respectively.[23] Further limitations were encountered when using hydroxyl- or cyano-substituted coupling partners.[24]

Importantly, the reaction was scalable and the same excellent results in terms of yield and selectivity were obtained when conducting the ruthenium catalyzed C–H bond amidation on a gram scale starting with 5 mmol of **1a** leading to *ca.* 1.30 g of product **3a**, thus showing the robustness of the methodology (Scheme 3).

For comparison purposes, the catalysis was applied to other substrates featuring cyclic amides as potential directing groups in a view to address the versatility of this transformation (Scheme 4). Using pyrrolidone, the simplest cyclic amide, as the directing group, afforded the corresponding *ortho*-C–H bond amidated product **4** in 60% yield (Scheme 4).

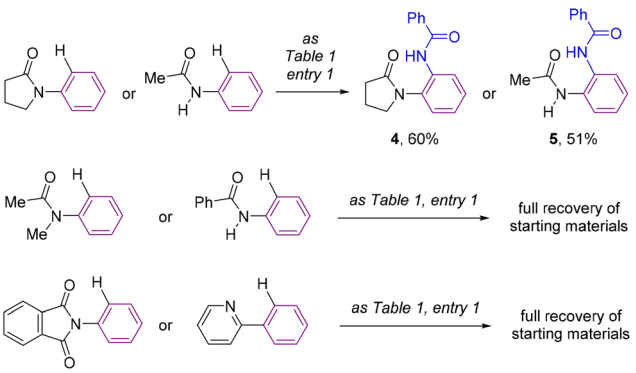

Scheme 4 Evaluation of the catalysis with different types of relevant directing groups.

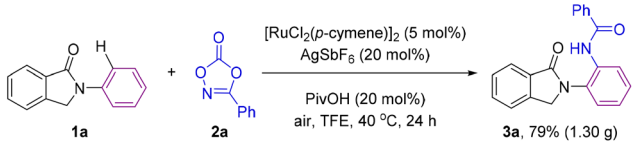

Scheme 3 Scale-up reaction for the ruthenium-catalyzed *ortho*-C–H bond amidation.

Note that the synthesis of **4** by applying this methodology was more sustainable and efficient compared to previous examples in the literature,[25] that required long and tedious reaction sequences using hazardous reagents that have so far limited their exploitation. Interestingly, a remarkable difference in reactivity was encountered exploiting acyclic amide directing groups. Indeed, whilst acetanilide still afforded the corres-

ponding *ortho*-amidated product **5** in 51% yield, no reactivity was observed for the *N*-methylated version or for benzanilide as the substrate (Scheme 4). Analogously, the complete absence of reactivity was encountered with *N*-phenylphthalimide, which features a cyclic imide as a potential directing group, as well as with the more strongly coordinating 2-pyridyl directing group (Scheme 4), which was rather counterintuitive considering previous contributions.[26]

Consequently, the reported ruthenium-catalyzed transformation appears to need a compromise between the geometry, the steric and electronic parameters, and the coordinating ability of the directing groups. Furthermore, these findings establish that the directing ability of cyclic amides outperforms that of acyclic amides following a clear trend as shown in Scheme 5.

After having demonstrated the enhanced efficiency of cyclic amides as superior directing groups in ruthenium-catalyzed aromatic C–H bond amidations, we performed several experiments to better understand the mechanism operating in the catalysis (Scheme 6). Firstly, we verified the necessity of the carbonyl group by attempting a catalytic reaction using a carbonyl-free substrate such as isoindoline (Scheme 6, top). In this case, no C–H bond functionalization was detected, indirectly demonstrating the importance of the carbonyl group in assisting the catalysis likely *via* coordination to ruthenium.[14,15] In addition, deuteration experiments were performed under the catalytic conditions but in the absence of the amidating partner **2** with a mixture of solvents TFE : D_2O (Scheme 6, bottom). Under these conditions, 17% deuteration incorporation was observed in the *ortho*-C–H bonds of the phenyl ring attached to the nitrogen atom with no deuteration observed elsewhere in the molecule (Scheme 6, bottom).

The overall above-described findings strongly suggest that cyclic amides prefer to accommodate six-membered ruthenacycle species in the catalytic cycle over commonly found five-membered ones for C–N bond forming reactions *via* C–H bond

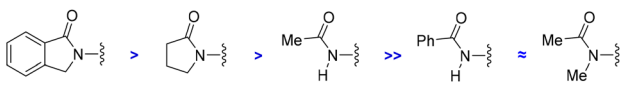

Scheme 5 Order of efficiency for amides as directing groups in ruthenium-catalyzed *ortho*-C–H bond amidations.

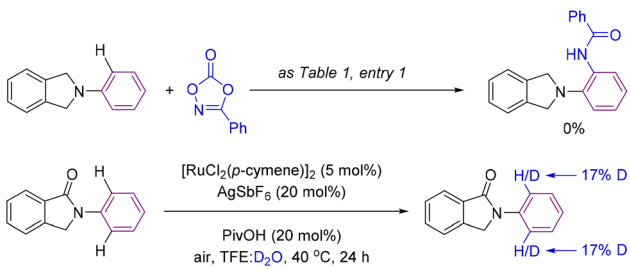

Scheme 6 Control experiment in the absence of a carbonyl directing group (top) and a deuteration experiment (bottom).

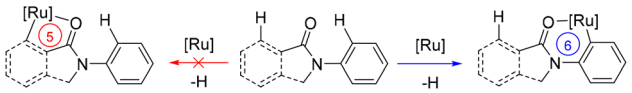

Scheme 7 Mechanistic consideration highlighting the stabilization of six-membered ruthenacycles over five-membered ones in the key C–H bond activation event.

activation (Scheme 7). This may account for the observed regio- and site-selectivity in the catalysis.

Due to the difficulty in obtaining reproducible data for kinetic studies ascribed to solubility issues and the unsuccessful attempts at detecting reaction intermediates, we turned our attention to further unveil the precise reaction mechanism (Fig. 1) by DFT computational calculations at the M06-D3/Def2TZVP~sdd(smd)//BP86-D3/Def2SVP level of theory.[24] In order to keep the whole reaction pathway at the same cationic level, the pre-activation started from the cationic intermediate **I0**, derived from $[RuCl_2(p\text{-cymene})]_2$, after releasing the chlorides by means of the reagent $AgSbF_6$ (a known halide scavenger). As such, SbF_6^- is considered the weak coordinating anion throughout the whole catalytic cycle. In the next intermediate **I0′** the anionic SbF_6^- ligand is substituted by the $PivO^-$ anion that comes from the other reagent, PivOH, with $HSbF_6$ release. This step is thermodynamically unfavoured by 13.1 kcal mol^{-1}, although the formation of complex **I0′** is essential to stabilize the intermediate **I0″** by 10.7 kcal mol^{-1} after the combination of **I0′** with substrate **1a**. From **I0″** there are two potential aryl C–H activations to explore: from the phenyl on the nitrogen or the aryl ring annulated to the five-membered ring.[27] Our simulations show energy barriers of 18.3 and 20.3 kcal mol^{-1}, respectively. Besides the 2 kcal mol^{-1} difference, the C–H bond activation of the aryl ring leads to a worsening of 9.7 kcal mol^{-1} for the resulting intermediate **I′** as compared to **I**, as is illustrated in the catalytic cycle in Fig. 1 (red pathway). The resulting ruthenacycle intermediate with the assistance of the cyclic amide as the directing group has literature precedents.[7,11–13]

In the catalytically productive pathway (Fig. 1, blue pathway), species **I** coordinates to dioxazolone forming species **II** followed by extrusion of CO_2, overcoming an energy barrier of 13.4 kcal mol^{-1} and giving rise to the formation of Ru^{IV}-imido species **III**. The migratory insertion of imido species **III**, with the associated C–N bond formation, leads to the generation of ruthenacycle **IV**, with a low energy barrier of only 8.4 kcal mol^{-1}. To close the catalytic cycle, the protodemetalation of species **IV** occurs with a new molecule of substrate **1**, which is in excess in the reaction mixture compared to the catalyst. This step could also be performed with $HSbF_6$ or PivOH, furnishing the amidated product, as well; however, instead of the regeneration of the active ruthenium catalyst **I**, the process would end up in intermediate **I0** or **I0′**, respectively.

The most difficult step in the pre-activation sequence is the C–H bond activation that leads to the ruthenacycle, either **I** or

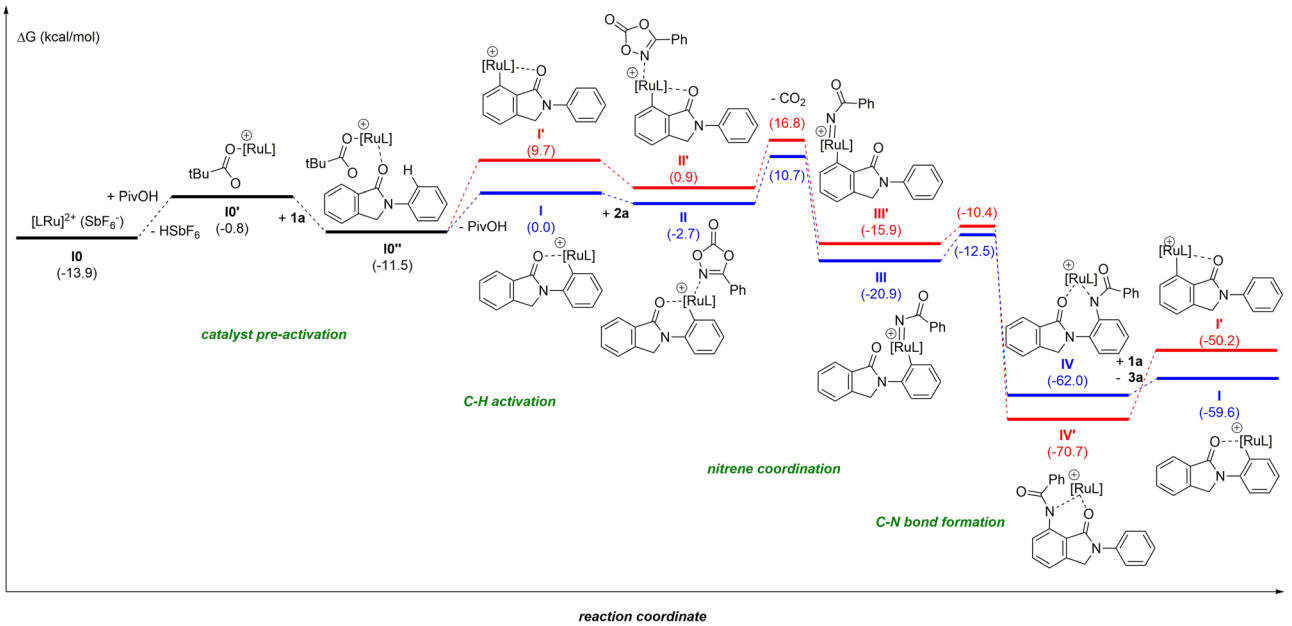

Fig. 1 Computed Gibbs energy reaction profile in kcal mol^{-1} (in brackets) of the ruthenium-catalyzed *ortho*-C–H bond amidation with cyclic amides as weak directing groups. L = *p*-cymene. Black pathway = catalyst pre-activation, red color = unfavoured pathway, and blue color = favoured pathway.

I′ selectively (Fig. 1). On the other hand, the rate determining step (rds) of the catalytic pathway corresponds to the transition state **II**-to-**III**. Considering the catalytic cycle for an elusive C–H bond activation at the aryl ring annulated to the five-membered ring of the substrate **1** (red pathway, Fig. 1), the corresponding transition state **II**-to-**III** is 6.1 kcal mol^{-1} higher in energy compared to the C–H bond activation at the phenyl ring linked to the nitrogen atom in **1** (blue pathway, Fig. 1). Thus, it confirms the selectivity towards the reaction profile with **I** as the catalytically active species. The reason is not steric hindrance, but it is related to the fact that **I** forms a rather stable 6-membered ruthenacycle, whereas **I′** has a 5-membered ruthenacycle (Fig. 2). In addition, in the transition state the pivalate ligand forms a less strained interaction to remove the proton, and actually the distances in the transition state leading to **I** are closer to an agostic interaction, with a more activated aryl C–H bond (by nearly 0.1 Å).

For the sake of consistency and to validate mainly the rds, we explored all the possibilities considering the intermediates in the pre-activation and the two substrates. Interestingly, from intermediate **I0′** the coordination of the dioxazolone before **1** is omitted since the kinetic cost of the CO_2 release increases by 5.3 kcal mol^{-1} (Fig. 3). Such findings strongly contrast with the initial elementary steps of the reaction mechanism associated with the ruthenium-catalyzed C–H bond amidation with azides, in which the ruthenium-nitrene species are postulated to form before the C–H bond activation step in the substrate.[28]

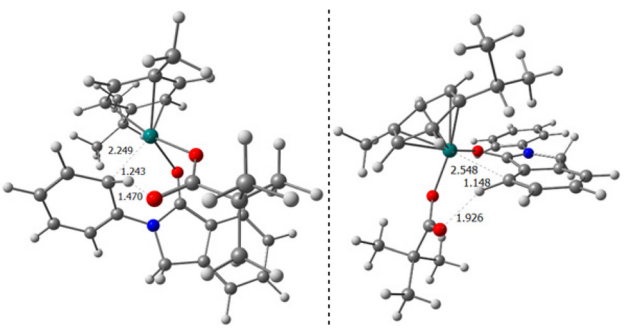

Fig. 2 Transition states **I0′′** → **I** (left) and **I0′′** → **I′** (right) with selected distances given in Å.

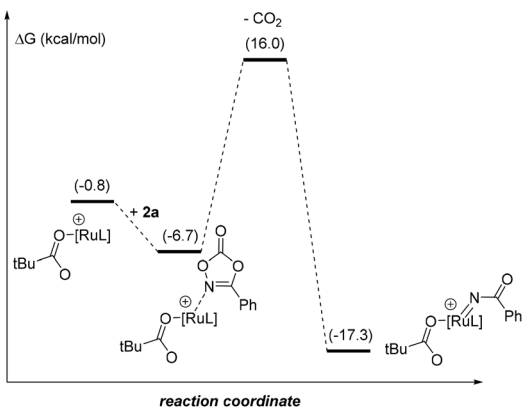

Fig. 3 Reaction profile of the extrusion of CO_2 with the coordination of dioxazolone in **I0′**. Relative Gibbs energies relative to **I** (in kcal mol^{-1}). L = *p*-cymene.

To further check the importance of the different anions, we performed additional analyses with the initial $[RuCl_2(p\text{-cymene})]_2$. The stability of this dimer is not relevant as its cleavage only requires 1.1 kcal mol^{-1}. The substitution of one or both chlorides by SbF_6^- is affordable, consuming only 3.1 and 2.8 kcal mol^{-1}, respectively. Moreover, for the reaction profile described in Fig. 1, the counter anion SbF_6^-, that would neutralize the system, was omitted assuming that it does not affect significantly. Preliminary calculations show that the counter anion destabilizes intermediates **I** and **II** by 4.1 and 0.5 kcal mol^{-1}, respectively.

Conclusions

In summary, we have developed efficient site-selective C–H bond amidation reactions to form unprecedented C–N bonds by exploiting the directing group ability of cyclic amides *via* six-membered ruthenacycle formation. A simple ruthenium(II) pre-catalyst and a safe amidating agent have been employed leading to a versatile catalytic system compatible with a large number of synthetically useful functional groups (more than 20 examples). This "close to room temperature" methodology offers a convenient route to access *ortho*-amidated cyclic amides that might be potentially relevant in medicinal chemistry.[16] This study also shows the subtlety associated with C–H bond amidations because in the present case ruthenium outperforms cobalt as a catalyst and dioxazolone outperforms tosylazide as an amidating agent, respectively, which is somehow unexpected with regard to precedents in the literature.[6–13,28] Moreover, this contribution establishes that cyclic amides are more powerful directing groups than acyclic ones or other coordinating groups such as imides and pyridines, at least for ruthenium-catalyzed C–H bond amidations. In addition, we provide the first mechanistic considerations of ruthenium-catalyzed C–H bond aminations supported by in-depth DFT calculations. Although the rate-determining step is the extrusion of CO_2 in order to form ruthenium species coordinated to both the substrate and nitrene group, the site-selective step is determined by the destabilization associated with the formation of a five-membered ruthenacycle over a six-membered one. In conclusion, further research directed to new carbon–heteroatom bond forming processes *via* ruthenium-catalyzed C–H bond functionalization strategies should provide appealing methodologies for direct implementation into organic synthesis.

Experimental

General procedure for the ruthenium-catalyzed C–H bond amidation

A suspension of substrate **1** (0.3 mmol, 1.0 equiv.), dioxazolone **2** (0.45 mmol, 1.5 equiv.), $[RuCl_2(p\text{-cymene})]_2$ (5 mol%), $AgSbF_6$ (20 mol%), and PivOH (0.06 mmol, 0.2 equiv.) in anhydrous TFE (1.5 mL) was stirred at 40 °C for 20 hours under air. At ambient temperature, the solvent was evaporated *in vacuo*, and the resulting crude reaction mixture was purified by flash column chromatography to afford the corresponding products **3–5** as analytically pure solids.

Computational details

All the DFT static calculations were performed with the Gaussian16 set of programs,[29] using the BP86 functional of Becke and Perdew,[30–32] together with the Grimme D3 correction term to the electronic energy.[33] The electronic configuration of the molecular systems was described with the double-ζ basis set with polarization of Ahlrichs for main-group atoms (Def2SVP keyword in Gaussian),[34] whereas for ruthenium the small–core quasi–relativistic Stuttgart/Dresden effective core potential with an associated valence basis set (standard SDD keywords in Gaussian16) was employed.[35–37] The geometry optimizations were performed without symmetry constraints, with analytical frequency calculations for the characterization of the located stationary points. These frequencies were used to calculate unscaled zero-point energies (ZPEs) as well as thermal corrections and entropy effects at 298.15 K. Energies were obtained by single-point calculations on the optimized geometries with the M06 functional,[38] with the Grimme D3 correction term[33] and the Def2TZVP basis set.[39] The reported Gibbs energies in this work contain electronic energies obtained at the M06-D3/Def2TZVP~sdd level of theory corrected with zero-point energies, thermal corrections and entropy effects evaluated at 298.15 K, achieved at the BP86-D3/Def2SVP~sdd level plus a solvation contribution evaluated by means of the SMD continuum solvation model based on the quantum mechanical charge density of the solute interacting with a continuum description of the solvent (2,2,2-trifluoroethanol, TFE).[40]

Conflicts of interest

There are no conflicts to declare.

Author contributions

Y–C. Y., Q.-L. L. and X.-T. Z. performed all syntheses, product characterization and catalysis. S. P.-P., M. S. and A. P. performed DFT computational calculations. T. R. performed X-ray diffraction studies. Y.-C. Y. and R. G.-D. conceptualized and directed the study. All authors contributed to manuscript writing.

Acknowledgements

Y.-C. Y. acknowledges the Science and Technology of XuZhou (KC19042) for financial support. We also thank the Public Experimental Research Center, Xuzhou Medical University, for NMR determination. R. G-D. acknowledges the ANR-JCJC scheme (ANR-19-CE07-0039), CNRS and the University of

Rennes 1 for financial support. S. P. P. thanks the Marie Curie fellowship (H2020-MSCA-IF-2020-101020330). A. P. is a Serra Húnter Fellow and thanks ICREA Academia Prize 2019 and Spanish Mineco for project ref. PGC2018-097722-B-I00. A. P. and M. S. thank the Spanish Ministerio de Ciencia e Innovación for projects PID2021-127423NB-I00 and PID2020-13711GB-I00 and the Generalitat de Catalunya for project 2017SGR39.

References

1 (*a*) P. Knochel and G. Molander, *Comprehensive Organic Synthesis*, Elsevier, Amsterdam, 2nd edn, 2014; (*b*) A. K. Yudin, *Catalyzed Carbon-Heteroatom Bond Formation*, Wiley-VCH, Weinheim, 2010; (*c*) A. R. Muci and S. L. Buchwald, Practical palladium catalysts for C-N and C-O bond formation, *Top. Curr. Chem.*, 2002, **219**, 131–209.

2 (*a*) N. R. Candeias, L. C. Branco, P. M. P. Gois, C. A. M. Afonso and A. F. Trindade, More sustainable approaches for the synthesis of *N*-based heterocycles, *Chem. Rev.*, 2009, **109**, 2703–2802; (*b*) R. Hili and A. K. Yudin, Making carbon-nitrogen bonds in biological and chemical synthesis, *Nat. Chem. Biol.*, 2006, **2**, 284–287.

3 F. Ullmann, Ueber eine neue Bildungsweise von Diphenylaminderivaten, *Ber. Dtsch. Chem. Ges.*, 1903, **36**, 2382–2384.

4 (*a*) F. Paul, J. Patt and J. F. Hartwig, Palladium-catalyzed formation of carbon-nitrogen bonds. Reaction intermediates and catalyst improvements in the hetero cross-coupling of aryl halides and tin amides, *J. Am. Chem. Soc.*, 1994, **116**, 5969–5970; (*b*) J. F. Hartwig, Evolution of a Fourth Generation Catalyst for the Amination and Thioetherification of Aryl Halides, *Acc. Chem. Res.*, 2008, **41**, 1534–1544; (*c*) A. S. Guram and S. L. Buchwald, Palladium-catalyzed aromatic aminations with in situ generated aminostannanes, *J. Am. Chem. Soc.*, 1994, **116**, 7901–7902; (*d*) D. S. Surry and S. L. Buchwald, Biaryl phosphane ligands in palladium-catalyzed amination, *Angew. Chem., Int. Ed.*, 2008, **47**, 6338–6361.

5 (*a*) F. Monnier and M. Taillefer, Catalytic C-C, C-N, and C-O Ullmann-Type Coupling Reactions, *Angew. Chem., Int. Ed.*, 2009, **48**, 6954–6971; (*b*) G. Evano, N. Blanchard and M. Toumi, Copper-mediated coupling reactions and their applications in natural products and designed biomolecules synthesis, *Chem. Rev.*, 2008, **108**, 3054–3131.

6 (*a*) F. Collet, R. H. Dodd and P. Dauban, Catalytic C-H amination: recent progress and future directions, *Chem. Commun.*, 2009, 5061–5074; (*b*) L. Van Emelen, M. Henrion, R. Lemmens and D. De Vos, C-N coupling reactions with arenes through C-H activation: the state-of-the-art versus the principles of green chemistry, *Catal. Sci. Technol.*, 2022, **12**, 360–389; (*c*) S. H. Cho, J. Y. Kim, J. Kwak and S. Chang, Recent advances in the transition metal-catalyzed twofold oxidative C-H bond activation strategy for C-C and C-N bond formation, *Chem. Soc. Rev.*, 2011, **40**, 5068–5083; (*d*) V. S. Thirunavukkarasu, S. I. Kozhushkov and L. Ackermann, C-H nitrogenation and oxygenation by ruthenium catalysis, *Chem. Commun.*, 2014, **50**, 29–39; (*e*) M.-L. Louillat and F. W. Patureau, Oxidative C-H amination reactions, *Chem. Soc. Rev.*, 2014, **43**, 901–910; (*f*) J. Jiao, K. Murakami and K. Itami, Catalytic Methods for Aromatic C-H Amination: An Ideal Strategy for Nitrogen-Based Functional Molecules, *ACS Catal.*, 2016, **6**, 610–633; (*g*) J. L. Jeffrey and R. Sarpong, Intramolecular C(sp^3)-H amination, *Chem. Sci.*, 2013, **4**, 4092–4106; (*h*) T. A. Ramirez, B. Zhao and Y. Shi, Recent advances in transition metal-catalyzed sp^3 C-H amination adjacent to double bonds and carbonyl groups, *Chem. Soc. Rev.*, 2012, **41**, 931–942.

7 (*a*) F. Yu, W. Shen, Y. Sun, Y. Liao, S. Jin, X. Lu, R. He, L. Zhong, G. Zhong and J. Zhang, Ruthenium-catalyzed C-H amination of aroylsilanes, *Org. Biomol. Chem.*, 2021, **19**, 6313–6321; (*b*) X.-H. Hu, X.-F. Yang and T.-P. Loh, Chelation-Assisted Rhodium-Catalyzed Direct Amidation with Amidobenziodoxolones: C(sp^2)-H, C(sp^3)-H, and Late-Stage Functionalizations, *ACS Catal.*, 2016, **6**, 5930–5934; (*c*) Y. Park, K. T. Park, J. G. Kim and S. Chang, Mechanistic studies on the Rh(III)-mediated amido transfer process leading to robust C-H amination with a new type of amidating reagent, *J. Am. Chem. Soc.*, 2015, **137**, 4534–4542; (*d*) J. Y. Kim, S. H. Park, J. Ryu, S. H. Cho, S. H. Kim and S. Chang, Rhodium-catalyzed intermolecular amidation of arenes with sulfonyl azides via chelation-assisted C-H bond activation, *J. Am. Chem. Soc.*, 2012, **134**, 9110–9113; (*e*) J. Ryu, K. Shin, S. H. Park, J. Y. Kim and S. Chang, Rhodium-Catalyzed Direct C-H Amination of Benzamides with Aryl Azides: A Synthetic Route to Diarylamines, *Angew. Chem., Int. Ed.*, 2012, **51**, 9904–9908; (*f*) B. Zhou, J. Du, Y. Yang, H. Feng and Y. Li, Rh(III)-Catalyzed C-H Amidation with *N*-Hydroxycarbamates: A New Entry to *N*-Carbamate-Protected Arylamines, *Org. Lett.*, 2014, **16**, 592–595; (*g*) T. Ryu, J. Min, W. Choi, W. H. Jeon and P. H. Lee, Synthesis of 2-Aryl-2*H*-benzotrizoles from Azobenzenes and *N*-Sulfonyl Azides through Sequential Rhodium-Catalyzed Amidation and Oxidation in One Pot, *Org. Lett.*, 2014, **16**, 2810–2813; (*h*) H. Hwang, J. Kim, J. Jeong and S. Chang, Regioselective Introduction of Heteroatoms at the C-8 Position of Quinoline N-Oxides: Remote C-H Activation Using N-Oxide as a Stepping Stone, *J. Am. Chem. Soc.*, 2014, **136**, 10770–10776; (*i*) C. Zhou, J. Zhao, W. Guo, J. Jiang and J. Wang, *N*-Methoxyamide: An Alternative Amidation Reagent in the Rhodium(III)-Catalyzed C-H Activation, *Org. Lett.*, 2019, **21**, 9315–9319; (*j*) P. Patel and S. Chang, *N*-Substituted Hydroxylamines as Synthetically Versatile Amino Sources in the Iridium-Catalyzed Mild C-H Amidation Reaction, *Org. Lett.*, 2014, **16**, 3328–3331; (*k*) P. Lei and Y. Hailong, Chiral Phosphoric Acid Catalyzed Atroposelective C-H Amination of Arenes, *Chin. J. Org. Chem.*, 2020, **40**, 2167–2169.

8 (*a*) B. Berzina, I. Sokolovs and E. Suna, Copper-Catalyzed *para*-Selective C–H Amination of Electron-Rich Arenes, *ACS*

Catal., 2015, **5**, 7008–7014; (*b*) P. Wang, G.-C. Li, P. Jain, M. E. Farmer, J. He, P.-X. Shen and J.-Q. Yu, Ligand-Promoted *meta*-C–H Amination and Alkynylation, *J. Am. Chem. Soc.*, 2016, **138**, 14092–14099; (*c*) C. J. Whiteoak, O. Planas, A. Company and X. Ribas, A First Example of Cobalt-Catalyzed Remote C-H Functionalization of 8-Aminoquinolines Operating through a Single Electron Transfer Mechanism, *Adv. Synth. Catal.*, 2016, **358**, 1679–1688; (*d*) H. Sahoo, M. K. Reddy, I. Ramakrishna and M. Baidya, Copper-Catalyzed 8-Amido Chelation-Induced Remote C-H Amination of Quinolines, *Chem. – Eur. J.*, 2016, **22**, 1592–1596; (*e*) R. Zhao, Y. Yang, X. Wang, P. Ren, Q. Zhang and D. Li, An efficient nickel/silver co-catalyzed remote C–H amination of 8-aminoquinolines with azodicarboxylates at room temperature, *RSC Adv.*, 2018, **8**, 37064–37068; (*f*) Y. Yin, J. Xie, F.-Q. Huang, L.-W. Qi and B. Zhang, Copper-Catalyzed Remote C–H Amination of Quinolines with *N*-Fluorobenzenesulfonimide, *Adv. Synth. Catal.*, 2017, **359**, 1037–1042; (*g*) Y. Wang, S. Zhang, X. Feng, X. Yu, M. Yamaguchi and M. Bao, Palladium-Catalyzed *Para*-C–H Bond Amination of 2-Aryl Chloromethylbenzenes, *J. Org. Chem.*, 2022, **87**, 10531–10538.

9 (*a*) A. Greenberg, C. M. Breneman and J. F. Liebman, *The Amide Linkage: Structural Significance in Chemistry, Biochemistry, and Materials Science*, Wiley, New York, 2000; (*b*) E. Valeur and M. Bradley, Amide bond formation: beyond the myth of coupling reagents, *Chem. Soc. Rev.*, 2009, **38**, 606–631; (*c*) R. M. Lanigan and T. D. Sheppard, Recent Developments in Amide Synthesis: Direct Amidation of Carboxylic Acids and Transamidation Reactions, *Eur. J. Org. Chem.*, 2013, 7453–7465; (*d*) R. M. de Figuereido, J.-S. Suppo and J.-M. Campagne, Nonclassical routes for amide bond formation, *Chem. Rev.*, 2016, **116**, 12029–12122; (*e*) V. R. Pattabiraman and J. W. Bode, Rethinking amide bond synthesis, *Nature*, 2011, **480**, 471–479.

10 For reviews on amides as directing groups in transition metal-catalyzed C–H bond functionalization, see: (*a*) R.-Y. Zhu, M. E. Farmer, Y.-Q. Chen and J.-Q. Yu, A simple and versatile amide directing group for C–H functionalizations, *Angew. Chem., Int. Ed.*, 2016, **55**, 10578–10599; (*b*) R. Das, G. S. Kumar and M. Kapur, Amides as Weak Coordinating Groups in Proximal C–H Bond Activation, *Eur. J. Org. Chem.*, 2017, 5439–5459; (*c*) R. Gramage-Doria, Steering Site-Selectivity in Transition Metal-Catalyzed C–H Bond Functionalization: the Challenge of Benzanilides, *Chem. – Eur. J.*, 2020, **26**, 9688–9709; (*d*) R. Thakur, Y. Jaiswal and A. Kumar, Primary amides: Sustainable weakly coordinating groups in transition metal-catalyzed C–H bond functionalization reactions, *Tetrahedron*, 2021, **93**, 132313.

11 (*a*) J. Park and S. Chang, Comparative Catalytic Activity of Group 9 [Cp^*M^{III}] Complexes: Cobalt-Catalyzed C-H Amidation of Arenes with Dioxazolones as Amidating Reagents, *Angew. Chem., Int. Ed.*, 2015, **54**, 14103–14107; (*b*) G. N. Hermann and C. Bolm, Mechanochemical rhodium(III)-catalyzed C–H bond amidation of arenes with dioxazolones under solventless conditions in a ball mill, *ACS Catal.*, 2017, **7**, 4592–4596; (*c*) A. E. Hande and K. R. Prabhu, Ru(II)-Catalyzed C–H Amidation of Indoline at the C7-Position Using Dioxazolone as an Amidating Agent: Synthesis of 7-Amino Indoline Scaffold, *J. Org. Chem.*, 2017, **82**, 13405–13413; (*d*) J. Park, J. Lee and S. Chang, Iterative C–H functionalization leading to multiple amidations of anilides, *Angew. Chem., Int. Ed.*, 2017, **56**, 4256–4260; (*e*) Y. Hwang, Y. Park and S. Chang, Mechanism-Driven Approach To Develop a Mild and Versatile C–H Amidation through Ir^{III} Catalysis, *Chem. – Eur. J.*, 2017, **23**, 11147–11152; (*f*) H. Xiong, S. Xu, S. Sun and J. Cheng, Cp* Rh(III)-catalyzed annulation of N-methoxybenzamide with 1,4,2-bisoxazol-5-one toward 2-aryl quinazolin-4(3H)-one derivatives, *Org. Chem. Front.*, 2018, **5**, 2880–2884; (*g*) K. Kawai, Y. Bunno, T. Yoshino and S. Matsunaga, Weinreb Amide Directed Versatile C–H Bond Functionalization under (η^5-Pentamethylcyclopentadienyl)cobalt(III) Catalysis, *Chem. – Eur. J.*, 2018, **24**, 10231–10237; (*h*) Y. Liang, Y.-F. Liang, C. Tang, Y. Yuan and N. Jiao, Cationic Cobalt(III)-Catalyzed Aryl and Alkenyl C-H Amidation: A Mild Protocol for the Modification of Purine Derivatives, *Chem. – Eur. J.*, 2015, **21**, 16395–16399; (*i*) A. S. Santos, A. M. S. Silva and M. M. B. Marques, Sustainable amidation reactions–recent advances, *Eur. J. Org. Chem.*, 2020, 2501–2516; (*j*) K.-H. Ng, A. S. C. Chan and W.-Y. Yu, Pd-Catalyzed Intermolecular *ortho*-C–H Amidation of Anilides by *N*-Nosyloxycarbamate, *J. Am. Chem. Soc.*, 2010, **132**, 12862–12864.

12 (*a*) J. Ryu, J. Kwak, K. Shin, D. Lee and S. Chang, Ir(III)-Catalyzed Mild C–H Amidation of Arenes and Alkenes: An Efficient Usage of Acyl Azides as the Nitrogen Source, *J. Am. Chem. Soc.*, 2013, **135**, 12861–12868; (*b*) D.-G. Yu, M. Suri and F. Glorius, Rh^{III}/Cu^{II}-Cocatalyzed Synthesis of 1*H*-Indazoles through C–H Amidation and N–N Bond Formation, *J. Am. Chem. Soc.*, 2013, **135**, 8802–8805; (*c*) Y. Lian, J. R. Hummel, R. G. Bergman and J. A. Ellman, Facile Synthesis of Unsymmetrical Acridines and Phenazines by a Rh(III)-Catalyzed Amination/Cyclization/Aromatization Cascade, *J. Am. Chem. Soc.*, 2013, **135**, 12548–12551; (*d*) C. Pan, N. Jin, H. Zhang, J. Han and C. Zhu, Iridium-Catalyzed Phosphoramidation of Arene C–H Bonds with Phosphoryl Azide, *J. Org. Chem.*, 2014, **79**, 9427–9432; (*e*) J. Kim and S. Chang, Iridium-Catalyzed Direct C-H Amidation with Weakly Coordinating Carbonyl Directing Groups under Mild Conditions, *Angew. Chem., Int. Ed.*, 2014, **53**, 2203–2207; (*f*) N. Wang, R. Li, L. Li, S. Xu, H. Song and B. Wang, Rhodium(III)-Catalyzed Intermolecular Amidation with Azides via $C(sp^3)$–H Functionalization, *J. Org. Chem.*, 2014, **79**, 5379–5385; (*g*) D. Lee, Y. Kim and S. Chang, Iridium-Catalyzed Direct Arene C–H Bond Amidation with Sulfonyl- and Aryl Azides, *J. Org. Chem.*, 2013, **78**, 11102–11109; (*h*) T. M. Figg, S. Park, J. Park, S. Chang and D. G. Musaev, Comparative

Investigations of Cp*-Based Group 9 Metal-Catalyzed Direct C–H Amination of Benzamides, *Organometallics*, 2014, **33**, 4076–4085; (*i*) K. M. van Vliet and B. de Bruin, Dioxazolones: Stable Substrates for the Catalytic Transfer of Acyl Nitrenes, *ACS Catal.*, 2020, **10**, 4751–4769; (*j*) E. Tosi, R. M. de Figueiredo and J.-M. Campagne, Enantioselective Catalytic CH Amidations: An Highlight, *Catalysts*, 2021, **11**, 471; (*k*) S. Y. Hong, Y. Hwang, M. Lee and S. Chang, Mechanism-Guided Development of Transition-Metal-Catalyzed C–N Bond-Forming Reactions Using Dioxazolones as the Versatile Amidating Source, *Acc. Chem. Res.*, 2021, **54**, 2683–2700; (*l*) Y. Huang, C. Pi, Z. Tang, Y. Wu and X. Cui, Cp*Co(III)-catalyzed CH amidation of azines with dioxazolones, *Chin. Chem. Lett.*, 2020, **31**, 3237–3240; (*m*) K. Wei, M. Jiang, S. Liang and W. Yu, Iron-Catalyzed Benzene Ring Expansion of α-Azido-N-phenylamides, *Synthesis*, DOI: **10.1055/a-1915-7916**.

13 P. G. Chirila, L. Skibinski, K. Miller, A. Hamilton and C. J. Whiteoak, Towards a Sequential One-Pot Preparation of 1,2,3-Benzotriazin-4(3*H*)-ones Employing a Key Cp*Co (III)-catalyzed C–H Amidation Step, *Adv. Synth. Catal.*, 2018, **360**, 2324–2332.

14 For reviews on weak directing groups, see: (*a*) K. M. Engle, T.-S. Mei, M. Wasa and J.-Q. Yu, Weak coordination as a powerful means for developing broadly useful C–H functionalization reactions, *Acc. Chem. Res.*, 2012, **45**, 788–802; (*b*) S. De Sarkar, W. Liu, S. I. Kozhushkov and L. Ackermann, Weakly Coordinating Directing Groups for Ruthenium(II)-Catalyzed C–H Activation, *Adv. Synth. Catal.*, 2014, **356**, 1461–1479; (*c*) C. Sambiagio, D. Schoenbauer, R. Blieck, T. Dao-Huy, G. Pototschnig, P. Schaaf, T. Wiesinger, M. F. Zia, J. Wencel-Delord, T. Besset, B. U. W. Maes and M. Schnuerch, A comprehensive overview of directing groups applied in metal-catalysed C–H functionalisation chemistry, *Chem. Soc. Rev.*, 2018, **47**, 6603–6743.

15 (*a*) Y.-C. Yuan, M. Goujon, C. Bruneau, T. Roisnel and R. Gramage-Doria, C-H Bond Alkylation of Cyclic Amides with Maleimides via a Site-selective-determining Six-membered Ruthenacycle, *J. Org. Chem.*, 2019, **84**, 16183–61191; (*b*) Y.-C. Yuan, C. Bruneau, T. Roisnel and R. Gramage-Doria, Site-selective Ruthenium-catalyzed C-H Bond Arylations with Boronic Acids: Exploiting Isoindolinones as a Weak Directing Group, *J. Org. Chem.*, 2019, **84**, 12893–12903; (*c*) Y.-C. Yuan, C. Bruneau, T. Roisnel and R. Gramage-Doria, Site-selective Ru-catalyzed C–H bond alkenylation with biologically relevant isoindolinones: a case of catalyst performance controlled by subtle stereoelectronic effects of the weak directing group, *Catal. Sci. Technol.*, 2019, **9**, 4711–4717; (*d*) Y.-C. Yuan, C. Bruneau, T. Roisnel and R. Gramage-Doria, Ruthenium(II)-catalysed Selective C(sp^2)-H Bond Benzoxylation of Biologically Appealing *N*-arylisoindolinones, *Org. Biomol. Chem.*, 2019, **17**, 7517–7525; (*e*) Y.-C. Yuan, C. Bruneau, V. Dorcet, T. Roisnel and R. Gramage-Doria, Ru-catalyzed Selective C-H Bond Hydroxylation of Cyclic Imides, *J. Org. Chem.*, 2019, **84**, 1898–1907; (*f*) M. Xiong, Y. Shu, J. Tang, F. Yang and D. Xing, Iridium(I)-Catalyzed Isoindolinone-Directed Branched-Selective Aromatic C–H Alkylation with Simple Alkenes, *Molecules*, 2022, **27**, 1923.

16 (*a*) S. Nomura, K. Endo-Umeda, A. Aoyama, M. Makishima, Y. Hashimoto and M. Ishikawa, Styrylphenylphthalimides as novel transrepression-selective liver X receptor (LXR) modulators, *ACS Med. Chem. Lett.*, 2015, **6**, 902–907; (*b*) S. Nomura, K. Endo-Umeda, M. Makishima, Y. Hashimoto and M. Ishikawa, Development of Tetrachlorophthalimides as Liver X Receptor β (LXRβ)-Selective Agonists, *ChemMedChem*, 2016, **11**, 2347–2360; (*c*) S. Nomura, K. Endo-Umeda, S. Fujii, M. Makishima, Y. Hashimoto and M. Ishikawa, Structural development of tetrachlorophthalimides as liver X receptor β (LXRβ)-selective agonists with improved aqueous solubility, *Bioorg. Med. Chem. Lett.*, 2018, **28**, 796–801; (*d*) M. R. Lunn, D. E. Root, A. M. Martino, S. P. Flaherty, B. P. Kelley, D. D. Coovert, A. H. Burghes, N. T. Man, G. E. Morris, J. Zhou, E. J. Androphy, C. J. Sumner and B. R. Stockwell, Indoprofen upregulates the survival motor neuron protein through a cyclooxygenase-independent mechanism, *Chem. Biol.*, 2004, **11**, 1489–1493; (*e*) D. W. Beight, T. J. Craft, J. B. Franciskovich, T. Goodson Jr., S. E. Hall, D. K. Herron, V. J. Klimkowski, J. A. Kyle, J. J. Masters, D. Mendel, G. Milot, J. S. Sawyer, R. T. Shuman, G. F. Smith, A. L. Tebbe, J. M. Tinsley, L. C. Weir, J. H. Wikel, M. R. Wiley and J. K. Yee, Preparation of bis-amides of 1,2-benzenediamines as antithrombotic agents, 1998, WO1998-US13427.

17 (*a*) J. Yamaguchi, A. D. Yamaguchi and K. Itami, C-H Bond Functionalization: Emerging Synthetic Tools for Natural Products and Pharmaceuticals, *Angew. Chem., Int. Ed.*, 2012, **51**, 8960–9009; (*b*) T. Brueckl, R. D. Baxter, Y. Ishihara and P. S. Baran, Innate and guided C–H functionalization logic, *Acc. Chem. Res.*, 2012, **45**, 826–839; (*c*) J. F. Hartwig, Evolution of C–H bond functionalization from methane to methodology, *J. Am. Chem. Soc.*, 2016, **138**, 2–24; (*d*) D. J. Abrams, P. A. Provencher and E. J. Sorensen, Recent applications of C–H functionalization in complex natural product synthesis, *Chem. Soc. Rev.*, 2018, **47**, 8925–8967; (*e*) R. Gramage-Doria and C. Bruneau, Ruthenium-catalysed oxidative coupling of vinyl derivatives and application in tandem hydrogenation, *Coord. Chem. Rev.*, 2021, **428**, 21362; (*f*) Q. Zheng, C.-F. Liu, J. Chen and G.-W. Rao, C–H functionalization of aromatic amides, *Adv. Synth. Catal.*, 2020, **362**, 1406–1446.

18 Prices accessed on September 1st 2022: iridium (4750 USD/OZ), rhodium (14 200 USD/OZ), palladium (2098 USD/OZ) and ruthenium (585 USD/OZ).

19 CCDC 2149748 (**3c**)† contains the supplementary crystallographic data for this paper.

20 (*a*) R. Manikandan and M. Jeganmohan, Recent advances in the ruthenium(ii)-catalyzed chelation-assisted C–H olefination of substituted aromatics, alkenes and heteroaromatics with alkenes *via* the deprotonation pathway, *Chem.*

Commun., 2017, **53**, 8931–8947; (*b*) R. Manikandan and M. Jeganmohan, Recent advances in the ruthenium-catalyzed hydroarylation of alkynes with aromatics: synthesis of trisubstituted alkenes, *Org. Biomol. Chem.*, 2015, **13**, 10420–10436; (*c*) Y. Yang, Y. Lin and Y. Rao, Ruthenium(II)-catalyzed synthesis of hydroxylated arenes with ester as an effective directing group, *Org. Lett.*, 2012, **14**, 2874–2877; (*d*) M. Pichette Drapeau and L. J. Goossen, Carboxylic acids as directing groups for C–H bond functionalization, *Chem. – Eur. J.*, 2016, **22**, 18654–18677; (*e*) G. Shi and Y. Zhang, Carboxylate-Directed C-H Functionalization, *Adv. Synth. Catal.*, 2014, **356**, 1419–1442.

21 (*a*) C. R. Le Blond, A. T. Andrews, Y. Sun and J. R. Sowa, Activation of aryl chlorides for Suzuki cross-coupling by ligandless, heterogeneous palladium, *Org. Lett.*, 2001, **3**, 1555–1557; (*b*) P. Orecchia, D. S. Petkova, R. Goetz, F. Rominger, A. S. K. Hashmi and T. Schaub, Pd-Catalysed Suzuki–Miyaura cross-coupling of aryl chlorides at low catalyst loadings in water for the synthesis of industrially important fungicides, *Green Chem.*, 2021, **23**, 8169–8180; (*c*) R. A. Altman and S. L. Buchwald, Pd-catalyzed Suzuki–Miyaura reactions of aryl halides using bulky biarylmonophosphine ligands, *Nat. Protoc.*, 2007, **2**, 3115–3121.

22 H. J. Kim, M. J. Ajitha, Y. Lee, J. Ryu, J. Kim, Y. Lee, Y. Jung and S. Chang, Hydrogen-bond-assisted controlled C–H functionalization via adaptive recognition of a purine directing group, *J. Am. Chem. Soc.*, 2014, **136**, 1132–1140.

23 For the absence of reactivity using *ortho*-substituted patterns in C–H bond functionalizations assisted by cyclic amides as directing groups, see: (*a*) J. A. Leitch, P. B. Wilson, C. L. McMullin, M. F. Mahon, Y. Bhonoah, I. H. Williams and C. G. Frost, Ruthenium(II)-Catalyzed C–H Functionalization Using the Oxazolidinone Heterocycle as a Weakly Coordinating Directing Group: Experimental and Computational Insights, *ACS Catal.*, 2016, **6**, 5520–5529; (*b*) J. A. Leitch, H. P. Cook, Y. Bhonoah and C. G. Frost, Use of the Hydantoin Directing Group in Ruthenium(II)-Catalyzed C–H Functionalization, *J. Org. Chem.*, 2016, **81**, 10081–10087; (*c*) W. Ma, H. Dong, D. Wang and L. Ackermann, Late-Stage Diversification of Non-Steroidal Anti-Inflammatory Drugs by Transition Metal-Catalyzed C-H Alkenylations, Thiolations and Selenylations, *Adv. Synth. Catal.*, 2017, **359**, 966–973; and ref. 15.

24 See the ESI for details.†

25 (*a*) R. M. Anderson and D. Harrison, Methanesulphonyl and benzenesulphonyl derivatives of benzimidazolin-2-one, *J. Chem. Soc.*, 1964, 5231–5234; (*b*) O. Meth-Cohn, Acylation of benzimidazoles, *J. Chem. Soc.*, 1964, 5245–5247.

26 (*a*) J. McIntyre, I. Mayoral-Soler, P. Salvador, A. Poater and D. J. Nelson, Insights into mechanism and selectivity in ruthenium(II)-catalysed *ortho*-arylation reactions directed by Lewis basic groups, *Catal. Sci. Technol.*, 2018, **8**, 3174–3182; (*b*) D. S. Timofeeva, D. M. Lindsay, W. J. Kerr and D. J. Nelson, A quantitative empirical directing group scale for selectivity in iridium-catalysed hydrogen isotope exchange reactions, *Catal. Sci. Technol.*, 2020, **10**, 7249–7255.

27 For examples of activation of aryl C–H bonds in Ru-based catalysts, see: (*a*) J. A. Fernández-Salas, S. Manzini, L. Piola, A. M. Z. Slawin and S. P. Nolan, Ruthenium catalysed C–H bond borylation, *Chem. Commun.*, 2014, **50**, 6782–6784; (*b*) A. Poater, N. Bahri-Laleh and L. Cavallo, Rationalizing current strategies to protect *N*-heterocyclic carbene-based ruthenium catalysts active in olefin metathesis from C–H (de)activation, *Chem. Commun.*, 2011, **47**, 6674–6676; (*c*) A. Poater and L. Cavallo, Mechanistic insights into the double C–H (de)activation route of a Ru-based olefin metathesis catalyst, *J. Mol. Catal. A: Chem.*, 2010, **324**, 75–79; (*d*) I. Özdemir, S. Demir, B. Çetinkaya, C. Gourlaouen, F. Maseras, C. Bruneau and P. H. Dixneuf, Direct Arylation of Arene C–H Bonds by Cooperative Action of NHCarbene–Ruthenium(II) Catalyst and Carbonate via Proton Abstraction Mechanism, *J. Am. Chem. Soc.*, 2008, **130**, 1156–1157; (*e*) E. Ferrer Flegeau, C. Bruneau, P. H. Dixneuf and A. Jutand, Autocatalysis for C–H Bond Activation by Ruthenium(II) Complexes in Catalytic Arylation of Functional Arenes, *J. Am. Chem. Soc.*, 2011, **133**, 10161–10170.

28 I. Choi, A. M. Messinis and L. Ackermann, C7-Indole Amidations and Alkenylations by Ruthenium(II) Catalysis, *Angew. Chem., Int. Ed.*, 2020, **59**, 12534–12540.

29 M. J. Frisch, G. W. Trucks, H. B. Schlegel, G. E. Scuseria, M. A. Robb, J. R. Cheeseman, G. Scalmani, V. Barone, G. A. Petersson, H. Nakatsuji, X. Li, M. Caricato, A. V. Marenich, J. Bloino, B. G. Janesko, R. Gomperts, B. Mennucci, H. P. Hratchian, J. V. Ortiz, A. F. Izmaylov, J. L. Sonnenberg, D. Williams-Young, F. Ding, F. Lipparini, F. Egidi, J. Goings, B. Peng, A. Petrone, T. Henderson, D. Ranasinghe, V. G. Zakrzewski, J. Gao, N. Rega, G. Zheng, W. Liang, M. Hada, M. Ehara, K. Toyota, R. Fukuda, J. Hasegawa, M. Ishida, T. Nakajima, Y. Honda, O. Kitao, H. Nakai, T. Vreven, K. Throssell, J. A. Montgomery Jr., J. E. Peralta, F. Ogliaro, M. J. Bearpark, J. J. Heyd, E. N. Brothers, K. N. Kudin, V. N. Staroverov, T. A. Keith, R. Kobayashi, J. Normand, K. Raghavachari, A. P. Rendell, J. C. Burant, S. S. Iyengar, J. Tomasi, M. Cossi, J. M. Millam, M. Klene, C. Adamo, R. Cammi, J. W. Ochterski, R. L. Martin, K. Morokuma, O. Farkas, J. B. Foresman and D. J. Fox, *Gaussian 16, Revision C.01*, Gaussian, Inc., Wallingford CT, 2016.

30 A. Becke, Density-functional exchange-energy approximation with correct asymptotic behaviour, *Phys. Rev. A*, 1988, **38**, 3098–3100.

31 J. P. Perdew, Density-functional approximation for the correlation energy of the inhomogeneous electron gas, *Phys. Rev. B: Condens. Matter Mater. Phys.*, 1986, **33**, 8822–8824.

32 J. P. Perdew, Erratum: Density-functional approximation for the correlation energy of the inhomogeneous electron gas, *Phys. Rev. B: Condens. Matter Mater. Phys.*, 1986, **34**, 7406–7406.

33 S. Grimme, J. Antony, S. Ehrlich and H. A. Krieg, A consistent and accurate *ab initio* parametrization of density functional dispersion correction (DFT-D) for the 94 elements H-Pu, *J. Chem. Phys.*, 2010, **132**, 154104.
34 S. Schäfer, H. Horn and R. Ahlrichs, Fully optimized contracted Gaussian basis sets for atoms Li to Kr, *J. Chem. Phys.*, 1992, **97**, 2571–2577.
35 U. Haeusermann, M. Dolg, H. Stoll, H. Preuss, P. Schwerdtfeger and R. M. Pitzer, Accuracy of energy-adjusted quasirelativistic *ab initio* pseudopotentials: All-electron and pseudopotential benchmark calculations for Hg, HgH and their cations, *Mol. Phys.*, 1993, **78**, 1211–1224.
36 W. Küchle, M. Dolg, H. Stoll and H. Preuss, Energy-adjusted pseudopotentials for the actinides. Parameter sets and test calculations for thorium and thorium monoxide, *J. Chem. Phys.*, 1994, **100**, 7535–7542.
37 T. Leininger, A. Nicklass, H. Stoll, M. Dolg and P. Schwerdtfeger, The accuracy of the pseudopotential approximation. II. A comparison of various core sizes for indium pseudopotentials in calculations for spectroscopic constants of InH, InF, and InCl, *J. Chem. Phys.*, 1996, **105**, 1052–1059.
38 Y. Zhao and D. G. Truhlar, The M06 suite of density functionals for main group thermochemistry, thermochemical kinetics, noncovalent interactions, excited states, and transition elements: two new functionals and systematic testing of four M06-class functionals and 12 other functionals, *Theor. Chem. Acc.*, 2008, **120**, 215.
39 R. A. Kendall, T. H. Dunning Jr. and R. J. Harrison, Electron affinities of the first-row atoms revisited. Systematic basis sets and wave functions, *J. Chem. Phys.*, 1992, **96**, 6796–6806.
40 A. V. Marenich, C. J. Cramer and D. G. Truhlar, Universal Solvation Model Based on Solute Electron Density and on a Continuum Model of the Solvent Defined by the Bulk Dielectric Constant and Atomic Surface Tensions, *J. Phys. Chem. B*, 2009, **113**, 6378–6396.